

12-2011

Estimating oil concentration and flow rate with calibrated vessel-mounted acoustic echo sounders

Thomas C. Weber

University of New Hampshire, Durham, thomas.weber@unh.edu

Alex de Robertis

NOAA

Shep Smith

NOAA

Samuel F. Greenaway


NOAA

Larry A. Mayer

University of New Hampshire, larry.mayer@unh.edu

See next page for additional authors

Follow this and additional works at: <https://scholars.unh.edu/ccom>

 Part of the [Oceanography Commons](#), and the [Oil, Gas, and Energy Commons](#)

Recommended Citation

Weber, T. C. et al. Estimating oil concentration and flow rate with calibrated vessel-mounted acoustic echo sounders. *Proceedings of the National Academy of Sciences* 109, 20240–20245 (2011).

This Journal Article is brought to you for free and open access by the Center for Coastal and Ocean Mapping at University of New Hampshire Scholars' Repository. It has been accepted for inclusion in Center for Coastal and Ocean Mapping by an authorized administrator of University of New Hampshire Scholars' Repository. For more information, please contact nicole.hentz@unh.edu.

Authors

Thomas C. Weber, Alex de Robertis, Shep Smith, Samuel F. Greenaway, Larry A. Mayer, and Glen Rice

Estimating oil concentration and flow rate with calibrated vessel-mounted acoustic echo sounders

Thomas C. Weber^{a,1}, Alex De Robertis^b, Samuel F. Greenaway^c, Shep Smith^d, Larry Mayer^a, and Glen Rice^e

^aCenter for Coastal and Ocean Mapping, University of New Hampshire, 24 Colovos Road, Durham, NH 03824; ^bAlaska Fisheries Science Center, National Marine Fisheries Service, National Oceanic and Atmospheric Administration, 7600 Sand Point Way NE, Seattle, WA 98115; ^cJoint Hydrographic Center, National Oceanic and Atmospheric Administration, 24 Colovos Road, Durham, NH 03824; ^dNational Oceanic and Atmospheric Administration Ship *Thomas Jefferson*, Marine Operations Center Atlantic, National Oceanic and Atmospheric Administration, 439 York Street, Norfolk, VA 23510; and ^eCoast Survey Development Laboratory, National Oceanic and Atmospheric Administration, 1315 East West Highway, Silver Spring, MD 20910-3282

Edited by Marcia K. McNutt, US Geological Survey, Reston, VA, and approved October 5, 2011 (received for review June 10, 2011)

As part of a larger program aimed at evaluating acoustic techniques for mapping the distribution of subsurface oil and gas associated with the *Deepwater Horizon*-Macondo oil spill, observations were made on June 24 and 25, 2010 using vessel-mounted calibrated single-beam echo sounders on the National Oceanic and Atmospheric Administration ship *Thomas Jefferson*. Coincident with visual observations of oil at the sea surface, the 200-kHz echo sounder showed anomalously high-volume scattering strength in the upper 200 m on the western side of the wellhead, more than 100 times higher than the surrounding waters at 1,800-m distance from the wellhead, and weakening with increasing distance out to 5,000 m. Similar high-volume scattering anomalies were not observed at 12 or 38 kHz, although observations of anomalously low-volume scattering strength were made in the deep scattering layer at these frequencies at approximately the same locations. Together with observations of ocean currents, the acoustic observations are consistent with a rising plume of small (<1-mm radius) oil droplets. Using simplistic but reasonable assumptions about the properties of the oil droplets, an estimate of the flow rate was made that is remarkably consistent with those made at the wellhead by other means. The uncertainty in this acoustically derived estimate is high due to lack of knowledge of the size distribution and rise speed of the oil droplets. If properly constrained, these types of acoustic measurements can be used to rapidly estimate the flow rate of oil reaching the surface over large temporal and spatial scales.

Deepwater Horizon | oil plume | Gulf of Mexico | acoustic remote sensing

On April 20, 2010, an explosion on the *Deepwater Horizon* drilling rig precipitated an oil spill from a damaged wellhead located approximately 1,500-m below the sea surface, releasing an estimated $7.0 \times 10^5 \pm 20\%$ m³ (4.4×10^6 barrels) (1) to $7.82 \times 10^5 \pm 10\%$ m³ (4.92×10^6 barrels) (2) of oil and between 9.14×10^9 – 1.25×10^{10} mol of methane (3, 4) between April 22 and July 15, 2010 when the well was successfully capped. The depth of the damaged wellhead obscured our collective ability to observe what was happening to the oil as it exited the well, but by mid-May observations of underwater oil plumes were reported (e.g., ref. 5), and subsequent observations suggest that some portion of the spilled oil and methane remained in a deep plume (below 1,000 m) that was eventually advected hundreds of kilometers from the wellhead (3). The ability to account for the difference between the amount of oil exiting the wellhead and that arriving at the sea-surface is critical both in the short term as a guide to the response, providing a feedback mechanism that can be used to guide the dosage of subsea dispersant, for example, and in the long term in order to help determine the ecological impact of oil entering the Gulf of Mexico.

Several approaches have been taken to quantify the amount of oil exiting the wellhead during the spill including optical plume velocimetry derived from video taken at the wellhead, a methodology that resulted in an average estimated flow rate of $1.2 \times 10^{-1} \pm 20\%$ m³/s (6.8×10^4 barrels per day) after the riser

was removed (1), in close agreement to post-shut-in estimates made by Hsieh (2) which are regarded as the best estimate by the Flow Rate Technical Group (6). Camilli et al. (7) used a combination of a 1.8-MHz imaging sonar and a 1.2-MHz acoustic Doppler current profiler (ADCP) mounted on a remotely operated vehicle deployed at the wellhead, in addition to direct sampling of the oil and gas, to generate an estimate of $1.04 \times 10^{-1} \pm 0.018$ m³/s (57,000 barrels per day) on May 31, 2011 (prior to the removal of the riser), again in close agreement to Hsieh (2).

Quantifying the amount of oil reaching the surface has thus far been subject to higher uncertainties. For example, airborne remote-sensing techniques based on the wavelength-dependent absorption of near-infrared light were used to estimate the amount of oil on the surface on May 17, 2010. This estimate ranged from 66,000 to 500,000 barrels based on various assumptions including surface oil thickness (8). In order to provide estimates regarding the fate of the oil, the oil budget calculator used by the response team provided quantitative estimates of the amount of oil that was dispersed, but in order to do so, necessarily had to rely on the collective opinion of experts for which a consensus was never reached (9). Ryerson et al. (10) provided a more precise assessment of the flow rate based on the amount of hydrocarbons evaporating into the atmosphere using airborne measurements made on June 10, 2011. They estimated a surfacing fluid flow rate of 2.03×10^6 to 4.06×10^6 kg per day (15,100 to 30,200 barrels per day), not including fluid recovered to surface vessels from the cap on the wellhead, with the largest source of uncertainty attributed to uncertainties in the composition of hydrocarbons in the reservoir.

In this work, we present an additional methodology for quantifying the flux of oil to the surface based on acoustic observations of the surfacing oil plume made near the wellhead on June 24 and 25, 2010 on the National Oceanic and Atmospheric Administration (NOAA) ship *Thomas Jefferson*. We also present acoustic observations of anomalies in the deep scattering layer (DSL) in the near field of the wellhead that may offer some insight into the mechanics of the rising plume.

High-frequency (>10 kHz) acoustic methods utilizing vessel-mounted echo sounders, such as the ones used in this work, are frequently used to image marine organisms in the water column (11) but have also been used to observe controlled experimental discharges of oil and gas mixtures in the Norwegian Sea (12). One of the main advantages of using high-frequency shipboard echo sounders is their ability to generate a synoptic view of the ocean directly beneath the ship, creating an acoustic backscatter “map” extending from the ocean surface to the ocean bottom along the

Author contributions: T.C.W., A.D.R., S.F.G., S.S., L.M., and G.R. designed research; S.F.G. and S.S. performed research; T.C.W., A.D.R., and G.R. analyzed data; and T.C.W., A.D.R., S.F.G., and L.M. wrote the paper.

The authors declare no conflict of interest.

This article is a PNAS Direct Submission.

¹To whom correspondence should be addressed. E-mail: weber@ccom.unh.edu.

ship's track at normal ship transit speeds. When calibrated acoustic observations are coupled with knowledge of the nature of the acoustic scatterer (e.g., the size distribution of oil droplets and their acoustic scattering characteristics), quantitative assessments of the volume fraction of the scatterers within the water column can be made. These type of acoustic observations were made on the NOAA ships *Gordon Gunter*, *Thomas Jefferson*, *Pisces*, and *Henry Bigelow* from May–August 2010 in support of the *Deepwater Horizon* response efforts but, with the exception of the measurements made on the *Thomas Jefferson* at the end of June, these observations were made only outside of the rising oil plume.

Acoustic observations from all four NOAA ships made with the lower-frequency echo sounders (12, 18, and 38 kHz) often indicated the presence of methane seeps rising from the seafloor (13), a capability that was later exploited during wellhead integrity testing after the well was capped in mid-July (14). Gas bubbles in seawater strongly scatter sound, with scattering cross-sections that are several orders of magnitude higher than a similarly sized oil droplet at frequencies close to the mechanical resonance of the bubble (15). Both methane gas and oil were released from the damaged wellhead during the *Deepwater Horizon* spill, although only a minute portion (<0.01%) of the gas is thought to have been transported to the sea surface and released to the atmosphere (3, 10). The large difference in density between the oil and gas makes it likely that any portion of gas that did rise to the surface did so independently from the oil, and at much closer ranges to the wellhead than surfacing oil (16).

In this work, we describe acoustic measurements made over a period of approximately 10 h in the portion of the oil plume that was reaching the sea surface at distances between 1,800 and 5,000 m from the wellhead. The acoustic measurements were made with calibrated echo sounders operating at 12, 38, and 200 kHz. These acoustic measurements by themselves cannot provide an estimate of the flow rate of oil; they need to be coupled with knowledge of the droplet size distribution, the vertical velocity of the oil, and the acoustic properties of the oil (density and sound speed). Droplet size distributions were not made for the surfacing oil at the time of these measurements, making it difficult to accurately assess the flow rate. However, a rough approximation for the flow rate can be made using the

simplifying assumption that the droplets rose to the surface independently of one another and at their individual terminal velocity. The resulting uncertainty from this assumption is difficult to bound, but is likely to be a factor of two or more, and the main purpose in providing the estimate is to demonstrate how the acoustic measurements can be used to provide an estimate of the oil flow rate at the surface. The greatest contribution to the uncertainty in the results shown is the lack of knowledge of the droplet size distribution, a problem that could be remedied for future spills using optical techniques such as laser in situ scattering transmissometry (LISST) (17), other optical devices such as the shadowed image particle profiling and evaluation recorder (18), a broadband acoustic system (e.g., ref. 19), or some combination of these types of devices, at times and locations that are coincident with the acoustic measurements. It is worth noting that LISST measurements were made near the ocean surface during the spill, but they were focused on droplets with a radius smaller than 35 μm (9).

Observations of the Surfacing Oil Plume

During June 24 and 25, 2010, the *Thomas Jefferson* acoustically surveyed the water column at ranges between 1,800 and 5,000 m from the leaking wellhead using single-beam 12, 38, and 200 kHz Simrad ES60 echo sounders. Each of the echo sounders was calibrated on June 9, 2010 using the standard sphere method (20). The 200-kHz transducer (model 200-7) had a beamwidth of 7° and utilized a pulse length of 1 ms, and for this particular installation had a useful range of approximately 200 m. The 12- and 38-kHz transducers (models 12-16/60 and 38-7) had beamwidths of 16° and 7°, respectively, were operated with a pulse length of 1 ms prior to 03:51:30 on June 25, 2010 and 4 ms subsequently, and were able to image the entire water column.

During the acoustic survey, surfacing oil was visually observed on the west side of the wellhead by the ship's crew, and these visual observations were coincident with anomalously high returns from the 200-kHz ES60 at water depths shallower than 200 m, visible as narrow plumes with high-volume scattering strength (S_v in decibels with reference to 1 m^{-1} , or “re m^{-1} ”) in the vertically exaggerated echogram shown in Fig. 1A. The plumes were observed during a spiral survey pattern extending outward from the wellhead, with the anomaly confined only to

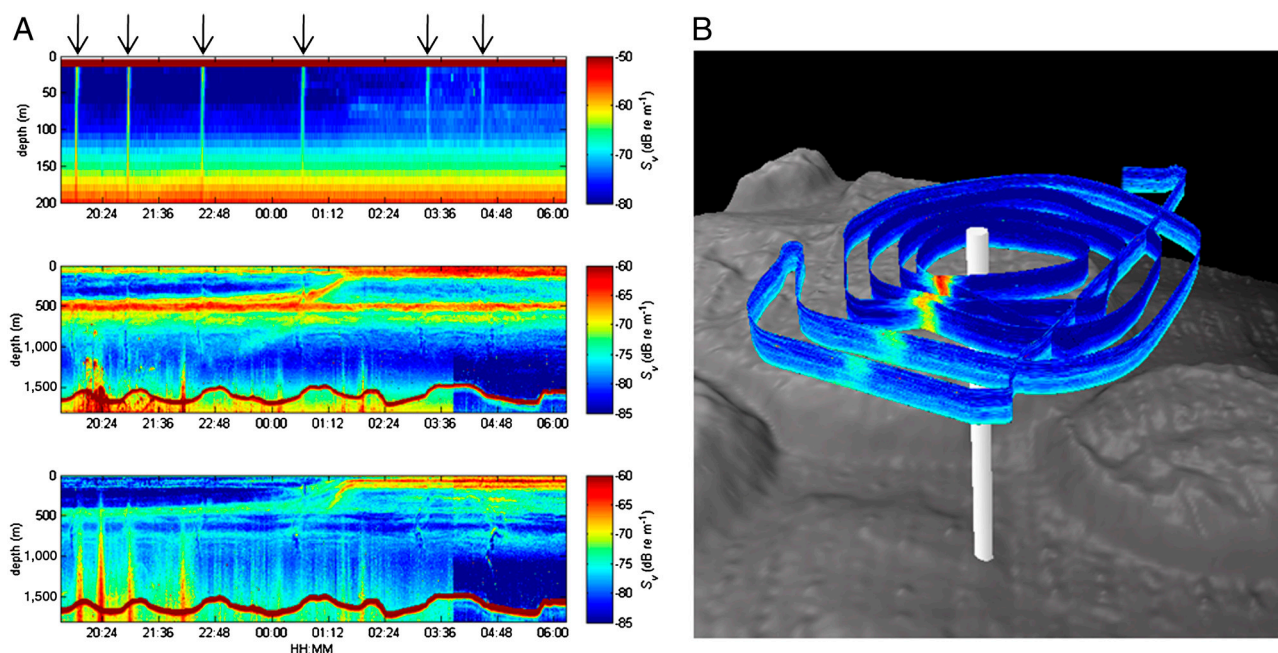


Fig. 1. (A) Echograms (S_v in decibels re m^{-1}) at 200 (Top), 38 (Middle), and 12 kHz (Bottom) on June 24 and 25, 2010 with arrows indicating the times of the plume crossings. (B) Georeferenced 200-kHz echograms and proximity to wellhead (white cylinder) with 6 \times vertical exaggeration.

the western side of the wellhead (closest point of approach, 1,800 m) and gradually weakening as the distance from the wellhead increased (Fig. 1B). At the closer ranges to the wellhead, the 200-kHz anomaly was visible to 200 m below the sea surface, at which range the echo sounder's range-dependent self-noise for this frequency increased to levels that masked the acoustic signals. The along-track length of the observed plume (i.e., the distance in the circumferential direction along the spiral survey) varied with distance from the wellhead, but was nominally 500 m.

Anomalous increases in S_V similar to the plumes observed in the 200-kHz ES60 data were not observed on either the 12- or 38-kHz ES60 data. Noise, often from the many other vessels around the wellhead, characterized by an S_V that monotonically increases with range and extends through the seafloor, is visible in both the 12- and 38-kHz data at depths greater than approximately 500 m, particularly at the closest ranges to the wellhead. Acoustic interference from other sonars (likely due to 38-kHz ADCPs on the rigs drilling relief wells) is visible in the 38-kHz ES60 data, particularly around 20:30 on 24 June. Acoustic scattering from the DSL, which is comprised of a diverse group of mesopelagic organisms (e.g., ref. 21) is visible between 400 and 1,000 m; a portion of the DSL migrates upward toward the surface just prior to sunset (02:34 on June 25, 2010). Although there is no clear 12- or 38-kHz oil signature coincident with the plumes observed at 200 kHz, there are anomalies in the scattered return from the DSL at these same plume locations (Fig. 2). These anomalies appear to have the morphology of a rising plume that sometimes extends from the base of the DSL to near the sea surface, but have a lower S_V than the surrounding waters except, occasionally, on the edges of the anomaly where the S_V is higher than would normally be expected for this area. The *Thomas Jefferson* transited this anomaly heading to the north on all transects shown except at 04:45 on June 25, 2010, which was observed while heading in a southerly direction. Based on the ship's track, the anomaly bends toward the south below 650 m and toward the north above 650 m. The cause of this mostly low S_V anomaly at 12 and 38 kHz is unknown, but could be due to a change in the acoustic reflectivity or distribution of marine organisms in this region caused by active avoidance, advection due to the rising oil, gas, and/or dispersants, either upstream or at the location of the observation, or a change in their scattering characteristics caused by the oil. Without direct sampling (e.g., net sampling or optical imaging) of the DSL organisms, the acoustic observations alone are unlikely to unambiguously determine the cause of this lower frequency anomaly.

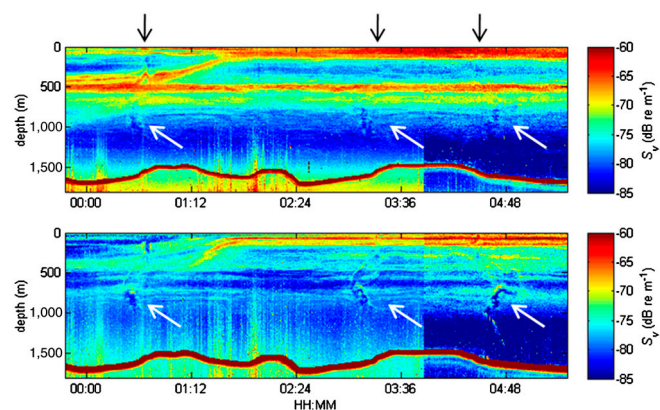


Fig. 2. Anomalies in the deep scattering layer observed on June 25 (Upper, 38 kHz; Lower, 12 kHz), with color corresponding to S_V in decibels re m^{-1} . The black arrows correspond to the times of anomalously high scattering levels observed at 200 kHz (Fig. 1). Decreased noise levels are evident after the pulse length is increased at 03:51. The rise to the surface of portions of the DSL is apparent from 00:30 to 02:00.

Both the observations of the surfacing oil and the anomalies in the DSL to the west of the wellhead are consistent with observations of currents made with a 38-kHz ADCP located on the *Discoverer Enterprise* drilling rig, which was supporting capping and containment activities near the Macondo well during the time of the measurements, and located within the spiral survey pattern. ADCP observations made between 00:00 June 24, 2010 and 04:50 June 25, 2010 show an average southwesterly current in the lower portion of the water column, becoming westerly between 650- and 1,100-m depth, and then turning toward the northwest above 650 m (current velocity data available at www.ndbc.noaa.gov, station 42868) (Fig. 3). The average of the westerly component of the current for these data is 3 cm/s, with substantial fluctuations (standard deviation equal to 3.3 cm/s). Ignoring the fluctuations for the sake of simplicity and assuming that the 3 cm/s current speed is valid for the entire water column, the observed oil would have required at least 17 h to be transported the distance of the first plume crossing (1,800 m from the wellhead) and at least 46 h to be transported to the last plume crossing (5,000 m from the wellhead). It is possible that the surfacing plume would have also been detectable at closer distances to the wellhead, but response operations precluded the *Thomas Jefferson* from making these observations.

During the time that the *Thomas Jefferson* was conducting the acoustic survey, the research vessel *Brooks McCall* was profiling the water column at fixed locations using a Wetlabs ECO Colored Dissolved Organic Matter (CDOM) fluorometer in addition to a standard suite of hydrocast sensors (e.g., temperature, salinity, and pressure sensors) (cruise data available at data.nodc.noaa.gov/DeepwaterHorizon/Ship/Brooks_McCall/ORR/Cruise_09). Fluorescence peaks were observed in the vicinity of the detected oil plume on the western side of the wellhead (Fig. 4), but only at depths greater than 1,000 m. Two of the profiles were collected in reported locations that overlapped the acoustic observations of the plume (B103 and B104) between 11:30 and 15:00 on June 24, approximately 5 h prior to the acoustic observations, but no fluorescence anomalies that were coincident with the 200-kHz plume observations were observed. Thus, although the *Brooks McCall* fluorescence observations are consistent with a deep oil plume heading to the west, they did not detect the surfacing oil. The limit of detection for oil with a Wetlabs ECO CDOM

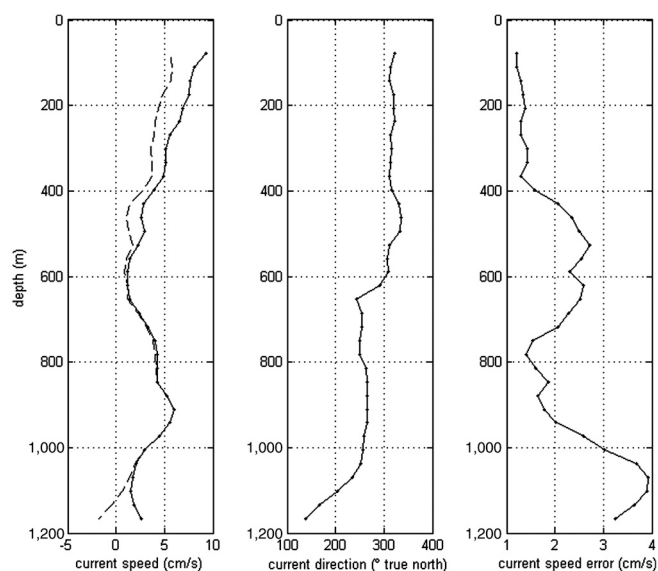


Fig. 3. Current observations made onboard the *Discoverer Enterprise* (26). (Left) Current speed (solid line) and current speed in westerly direction only (dashed line). (Center) Current direction. (Right) Average magnitude of the reported error in the horizontal current speed estimates.

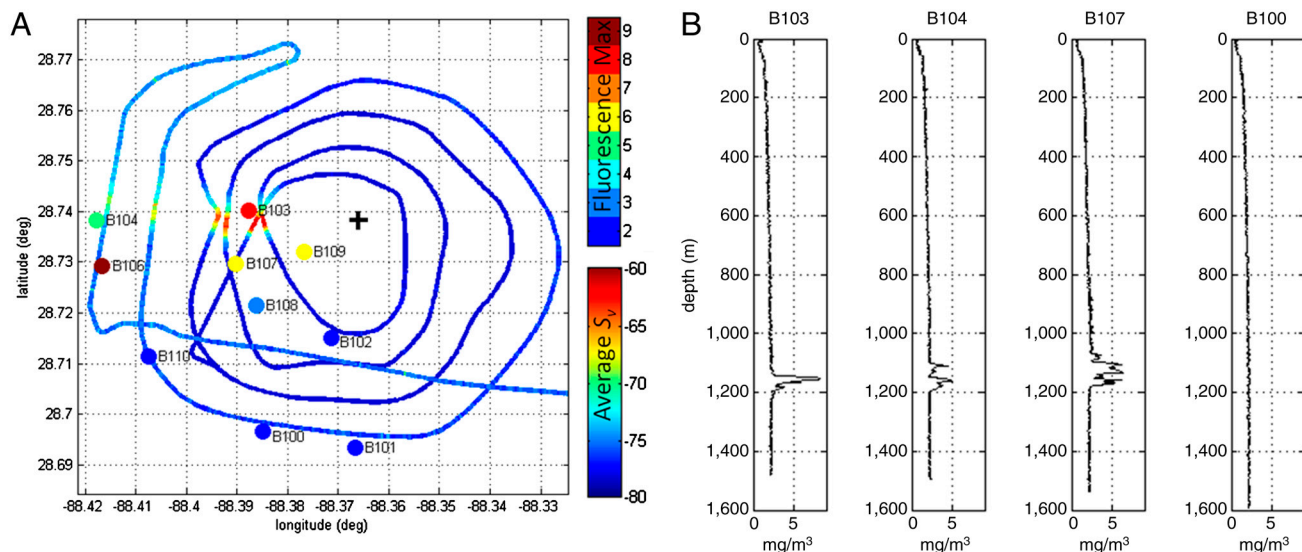


Fig. 4. (A) Locations and maximum of deepwater (>1,000 m) CDOM fluorescence (milligrams per cubic meter) anomalies observed by the *Brooks McCall* made on the June 24 and 25, 2010 (solid circles) (27) along with the shallower 200 kHz S_v (decibels re m^{-1}) averaged between 10- and 30-m depth along the *Thomas Jefferson's* ship track (colored line). The Macondo wellhead is shown as the black cross. (B) Examples of CDOM fluorescence profiles taken by the *Brooks McCall* (27).

fluorometer has been estimated to be 1 ppm (equivalent to a fluorometer output of 1.2 mg/m^3) for a dispersant to oil ratio of 1:25 (22). This detection limit is roughly equivalent to the fluorescence values that were ubiquitously observed in the upper 1,000 m (e.g., Fig. 3), suggesting that either the oil concentrations at the plume crossings were less than 1 ppm or that the hydrocasts were conducted near the edges or outside of the 500-m-wide plumes.

Estimating Oil Flux Using Acoustic Observations

The oil plume observed closest to the wellhead had an average S_v of approximately -60 dB re m^{-1} at 200 kHz, compared to a background level of approximately -80 dB re m^{-1} adjacent to the plume. At a similar depth, the observed S_v at 38 kHz (which was indistinguishable from the scattering from marine organisms outside of the oil plume at depths shallower than 200 m) was about -80 dB re m^{-1} , implying that the scattering strength for the oil within this plume was at least 20-dB stronger at 200 kHz than at 38 kHz. This increase in scattering strength with frequency is consistent with the idea that the observed oil is contained in small fluid droplets that are in the Rayleigh scattering regime, which occurs at values of $ka \ll 1$, where k is the acoustic wave number and a is the radius of an oil droplet. Spherical droplets of oil in this small ka limit have a total scattering cross-section, which is given by (23)

$$\sigma = 4\pi k^4 a^6 \left(\frac{\rho_w c_w^2}{3\rho_{oil} c_{oil}^2} - \frac{1}{3} + \frac{\rho_w - \rho_{oil}}{\rho_w + 2\rho_{oil}} \right)^2, \quad [1]$$

with a differential scattering cross-section in the backscatter direction equal to $\sigma/4\pi$, and where ρ_{oil} , ρ_w , c_{oil} , and c_w are the densities and compressional wave speeds in the oil and surrounding seawater, respectively. Rayleigh scatterers have a frequency-dependent scattering cross-section that is proportional to the fourth power of frequency, suggesting that the S_v at 200 kHz should be 29-dB higher than at 38 kHz, assuming that the Born (single scattering) approximation applies. This change in scattering strength would make the oil at this location within the plume unobservable for the reverberation-limited echo sounders operating at 12 or 38 kHz.

If the assumption that the oil droplets are in the Rayleigh scattering regime at 200 kHz (and below) is valid, the upper limit on the oil droplet radius occurs at $ka = 1$, or about a radius

of 1.2 mm. An oil droplet of this size would have likely taken approximately 4.8 h to rise to the surface, based on a terminal velocity of 8.7 cm/s in a water depth of 1,500 m using Table 1 and the formulation provided by Zheng and Yapa (24), or less if the oil rises partially through the water column as a buoyant plume. Using the average westerly component of the current speed of 3 cm/s, a 1.2-mm radius oil droplet would be transported approximately 520 m from the wellhead by the time it reaches the surface, making it likely that the observed oil was in droplets smaller than 1.2-mm radius, and supporting the assumption that the observed droplets were in the Rayleigh scattering regime.

If the oil in the rising plume was fractionated (25) and rising at the individual terminal velocity for single droplets from a depth of 1,500 m to the sea surface (neglecting the possibility of an increased vertical velocity caused by a buoyant plume, for simplicity), then the terminal velocity for droplets observed at a distance of 1,800 m from the wellhead (the first plume crossing in Fig. 1) would be 2.47 cm/s. For oil and seawater with the properties given in Table 1, this terminal velocity corresponds to an oil droplet with a radius of 389 μm . Assuming the rising oil is in a monodisperse population of this size, the number of droplets N per unit volume can be estimated as

$$N = 4\pi \frac{S_v}{\sigma}, \quad [2]$$

where $s_v = 10 \log_{10} S_v$. Using an estimate of the sound speed based on the observations of George et al. (26) for light oil and the parameters described in Table 1 along with ref. 1, the number of 393- μm -radius droplets required to generate an S_v of -60 dB re m^{-1} is 17,600, with an equivalent volume fraction of oil in the seawater equal to 4.3×10^{-6} . Maintaining the terminal rise speed

Table 1. Assumed properties of seawater and oil used for the calculation of the droplet terminal velocity, u_T , and the acoustic scattering cross-section, σ (9, 26; cruise data available at data.nodc.noaa.gov/DeepwaterHorizon/Ship/Brooks_McCall/ORR/Cruise_09)

	T , °C	S , PSU	ρ , kg/m ³	c , m/s	μ , Pa s
Seawater	15	35.9	1,027.6	1,511.4	0.0012
Oil	15	—	839	1,440.6	—

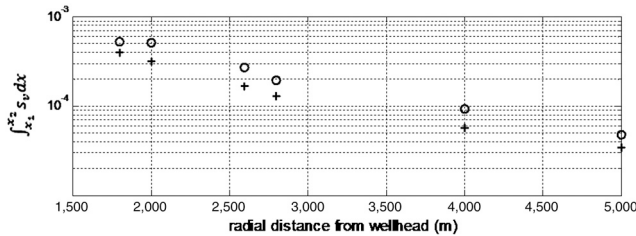


Fig. 5. Integrated s_v along each of the six plume crossings, averaged over depths between 10 and 30 m (circles) and 50 and 70 m (crosses).

of 2.47 cm/s for the droplets, the volume flux of oil at this location would be 1.1×10^{-7} m/s. The reverberation-limited noise floor is approximately -80 dB re m^{-1} during the day, increasing to -75 dB re m^{-1} at night with the change in the DSL. Assuming that a signal-to-noise ratio of 3 dB is required for detecting the oil, the detection limit in volume fraction of oil for 393- μm -radius droplets at 200 kHz is 8.7×10^{-8} during the day and 2.7×10^{-7} at night.

Integration of s_v along the ship track (i.e., in the circumferential direction) for an individual crossing and multiplication by the volume and rise speed for an individual droplet provides an estimate of the volumetric flow rate per unit radial distance, Q' :

$$Q' = u_T \frac{4}{3} \pi a^3 \int_{x_2}^{x_1} N dx = u_T \frac{16\pi^2}{3\sigma} a^3 \int_{x_2}^{x_1} s_v dx. \quad [3]$$

Eq. 3 is valid only for a monodisperse droplet size distribution. More generally, Q' would be found from a known (or measured) oil droplet size distribution $N\rho(a)$, where ρ is a probability density function describing the relative amount of droplets with radius a , from

$$\begin{aligned} Q' &= \int_0^\infty u_T(a) \frac{4}{3} \pi a^3 \rho(a) da \int_{x_2}^{x_1} N dx \\ &= \int_0^\infty u_T(a) \frac{16\pi^2}{3\sigma} a^3 \rho(a) da \int_{x_2}^{x_1} s_v dx. \end{aligned} \quad [4]$$

The flow rate of oil (cubic meters per second or barrels per day) would then be found by integrating [4] in the radial direction.

For the six plume crossings made by the *Thomas Jefferson*, the quantity $\int_{x_2}^{x_1} s_v dx$ is shown in Fig. 5, showing an approximately exponential decay in integrated volumetric scattering strength with increasing distance from the plume. Data from two depths are shown in Fig. 5, representing integrations of the average S_v between 10 and 30 m and between 50 and 70 m, and exhibiting an increase by a factor of approximately 1.5 at the shallower depth. These two depths were chosen because the integrated S_v (averaged over 5-m bins) showed two distinct layers with relatively consistent results both above and below 40 m. The cause of the higher scattering levels above 40 m is not known, but may be due to mixing and downward transport of oil from the surface (the mixed

layer depth was approximately 20 m; cruise data available at data.nodc.noaa.gov/DeepwaterHorizon/Ship/Brooks_McCall/ORR/Cruise_09), to ocean current variations, to variations in droplet size, or to the unsteady release of oil from the wellhead.

Neither $\rho(a)$ or u_T were measured at each of the plume crossings, so the flow rate for the observed portion of the oil plume cannot be accurately known. However, if a monodisperse droplet size distribution was assumed to be present at each plume crossing, with sizes defined by the terminal rise speed required for a droplet to stay below the sea surface from the wellhead out to the distances of the plume crossing, and accounting only for an average westerly current speed of 3 cm/s, [3] can be used in place of [4] to evaluate Q' (see Table 2). When Q' is estimated in this manner and then numerically integrated along the radial direction, the resulting flow rate estimate is 0.12 m³/s (62,000 barrels per day) for the observed portion of the plume at an average depth of 20 m and 0.076 m³/s (42,000 barrels per day) at an average depth of 60 m.

Both estimates for the surfacing oil based on the monodisperse droplet size distribution are remarkably similar to the estimate of the average flow rate at the wellhead made by Hsieh (2) for the same time period (i.e., after the riser was cut), but it is important to note that the uncertainty in the acoustically derived estimate is difficult to quantify primarily due to the assumptions regarding the droplet size. For the size range of droplets assumed to be present in this work ($a < 1$ mm), the rise time is proportional to the projected area of the droplet ($u_T \propto a^2$), and the flow rate is proportional to the inverse of the droplet size (i.e., $Q' \propto a^{-1}$). Thus, an overestimate in droplet size would imply an underestimate in the flow rate. If size estimates of the oil droplets in the plume were uniformly biased low by a factor of two, the flow rate estimate at 60-m depth would change to 0.04 m³/s (21,000 barrels per day). Further, the ADCP data shown in Fig. 3 only provide current data between 80 and 1,200 m, and our estimate of 3 cm/s westerly current in the lower 300 m may be erroneous; we have also ignored spatiotemporal fluctuations in the currents that may have sped or slowed the droplets along their path to the surface. Our estimates are based on an underlying assumption that the terminal rise velocity for individual droplets dominates the vertical transport throughout the entire water column. The estimates assume that the dynamics governing the jet and buoyant plume exiting the well act over a negligible portion of the water column from the perspective of vertical transport, an assumption that is consistent with the plume height results modeled by Yapa and Chen (27). Vertical ocean currents are also neglected, but could play an important role considering the low terminal velocities (0.5–3 cm/s) of the droplets assumed to be present in the plume. It is important to note that all of the sources of uncertainty associated with the droplet size listed here would be eliminated if measurements of the droplet size distribution were made in the surfacing plume at the same time as the acoustic observations were made.

Uncertainty in the acoustic measurements (Fig. 5) also contributes to the uncertainty in the flow rate estimate. The calibration of a single-beam 200-kHz ES60 estimates an on-axis gain, and

Table 2. Estimates of the flow rate per unit radial distance, and the intermediate quantities used to calculate it, for each plume crossing

Plume crossing	Distance from wellhead, m	u_T , cm/s		a , μm		σ , $\times 10^{-12}$ m ²		Q'	
								$\times 10^{-5}$ m ³ /s	
1	1,800	2.47	2.40	389	381	714	630	5.53	4.42
2	2,000	2.22	2.16	360	353	449	399	6.16	3.93
3	2,600	1.71	1.66	290	283	123	106	4.84	3.10
4	3,800	1.58	1.55	273	268	85.3	76.4	3.86	2.63
5	4,000	1.11	1.08	212	208	18.7	16.7	2.74	1.74
6	5,000	0.89	0.86	184	181	8.00	7.25	1.72	1.26

Two scenarios are examined based on acoustic observations at 20 m (first column) and 60 m (second column) depths.

the conversion of the raw measurements into volume scattering strength assumes a nominal equivalent beam angle, which together are likely to be accurate to within 25% for the equipment used. This uncertainty translates directly into an uncertainty in the flow rate estimate because the estimate of flow rate is proportional to the acoustic measurements [4]. Calibration uncertainty can be reduced to <10% with more quantitative echo sounders, such as those specially designed for fish abundance surveys (11).

Conclusions

Oil well blowouts in deep water, including the 83-d-long disaster at the 1,500-m-deep Macondo wellhead in the spring and summer of 2010, present observational challenges when trying to determine the fate of the oil. Understanding this fate is important to both aid response efforts and as a potential forcing function for long-term ecological consequences. High-frequency acoustic observations from vessel-mounted scientific echo sounders, such as the ones used in this work, can be used as part of a quantitative assessment of the flow rate for the oil reaching the ocean surface when coupled with knowledge of the droplet size distribution and rise velocity. For the acoustic observations made by the *Thomas Jefferson*, the droplet sizes were not observed, so a simple model was used to estimate the droplet size at each of the plume crossings. The resulting flow rate estimates of surfacing oil derived here are 1.5–4 times higher than those found from Ryerson et al. (10), the most precise estimate published to date, but it would be incorrect to assume that the rate estimates presented here are inconsistent with theirs. We attribute the difference in these

two measurements to a lack of accurate knowledge of the size distribution and rise speed of the acoustically observed droplets, information that is vital for relating the acoustic observations described here to an accurate flow rate estimate. Responders to future oil spills would be wise to directly measure the droplet size distributions and rise speeds at locations and times that are coincident with the acoustic measurements in order to substantially reduce the uncertainties of the final estimates.

Synoptic acoustic measurements such as those made by the *Thomas Jefferson* can be made relatively quickly: Six passes over the plume were made in less than 10 h during the spiral survey discussed here; if the plume location is constrained to one side of the wellhead, a set of acoustic measurements adequate for estimating the flow rate of surfacing oil could likely be made in only a few hours. The acoustic measurements make operational daily estimates of the surfacing flow achievable, providing information regarding the efficacy of subsea dispersants in response to changes in application and an estimate of the cumulative quantity of oil reaching the surface that could be subtracted from estimates of the flow from the wellhead itself in order to estimate the quantity of oil entering the deep ocean.

ACKNOWLEDGMENTS. We would like to acknowledge Sam Walker and the subsurface monitoring unit for their valuable assistance and guidance during this and other cruises conducted as part of the response to the *Deepwater Horizon*-Macondo oil spill. We would also like to acknowledge the crew of the *Thomas Jefferson* for their help during the collection of the acoustic data, as well as the science party and crew of the *Brooks McCall* for collecting oceanographic data near the wellhead during June 24 and 25. This work was supported under NOAA Grant NA05N054001153.

- Crone T, Tolstoy M (2010) Magnitude of the 2010 Gulf of Mexico oil leak. *Science* 330:634.
- Hsieh P (2010) Computer simulation of reservoir depletion and oil flow from the Macondo well following the *Deepwater Horizon* blowout. *US Geological Survey Open-File Report 2010-1266* pp 1–18.
- Kessler J, et al. (2011) A persistent oxygen anomaly reveals the fate of spilled methane in the deep Gulf of Mexico. *Science* 331:312–315.
- Valentine D, et al. (2010) Propane respiration jump-starts microbial response to a deep oil spill. *Science* 330:208–211.
- Camilli R, et al. (2010) Tracking hydrocarbon plume transport and biodegradation at deepwater horizon. *Science* 330:201–204.
- McNutt M, et al. (2012) Assessment of flow rate estimates for the *Deepwater Horizon*/Macondo well oil spill. *Flow Rate Technical Group report to the National Incident Command, Interagency Solutions Group* pp 1–22.
- Camilli R, et al. (2012) Acoustic measurement of the *Deepwater Horizon* Macondo well flow rate. *Proc Natl Acad Sci USA* 109:20235–20239.
- Clark R, et al. (2010) A method for quantitative mapping of thick oil spills using imaging spectroscopy. *US Geological Survey Open-File Report 2010-1167* pp 1–51.
- Federal Interagency Solutions Group, Oil Budget Calculator Science and Engineering Team (November 2010) Oil budget calculator: *Deepwater Horizon* technical documentation.
- Ryerson T, et al. (2012) Atmospheric emissions from the *Deepwater Horizon* spill constrain air-water partitioning, hydrocarbon fate, and leak rate. *Geophys Res Lett* 38:L07803.
- Simmonds E, MacLennan D (2005) *Fisheries Acoustics* (Blackwell Science, Oxford, UK), 2nd Ed., pp 70–126.
- Johansen O, Rye H, Cooper C (2003) DeepSpill—field study of a simulated oil and gas blowout in deep water. *Spill Sci Technol Bull* 8:433–443.
- Smith S, et al. (2010) NOAA ship *Thomas Jefferson* *Deepwater Horizon* Response Mission Report: Interim Project Report-Leg 2, June 3–11, 2010. (National Oceanic and Atmospheric Administration, Marine Operations Center Atlantic, Norfolk, VA), Available at: www.noaa.gov/scienceemissions/PDFs/tj_deepwaterhorizon_responseemissionreport_june3_11_2010final.pdf.
- Hickman S, et al. (2012) Scientific basis for safely shutting in the Macondo well following the April 20, 2010, *Deepwater Horizon* blowout. *Proc Natl Acad Sci USA* 109:20268–20273.
- Clay C, Medwin H (1977) *Acoustical Oceanography: Principles and Applications* (Wiley, New York), pp 194–203.
- Zheng L, Yapa P, Chen F (2003) A model for simulating deepwater oil and gas blowouts. Part I: Theory and model formulation. *J Hydraul Eng* 41:339–351.
- Agrawal Y, Pottsmith H (1994) Laser diffraction particle sizing in STRESS. *Continental Shelf Res* 14:1101–1121.
- Samson S, et al. (2001) A system for high-resolution zooplankton imaging. *IEEE J Oceanic Eng* 26:671–676.
- Lavery A, Chu D, Moum J (2010) Measurements of acoustic scattering from zooplankton and oceanic microstructure using a broadband echosounder. *ICES J Mar Sci* 67:379–394.
- Foote K, Knudsen H, Vestnes G, MacLennan D, Simmonds E (1987) Calibration of acoustic instruments for fish density estimation. *Coop Res Rep Int Councl Explor Sea* 144:1–69.
- Hopkins T, Landcraft T (1984) The composition and standing stock of mesopelagic micronekton at 27°N 86°W in the eastern Gulf of Mexico. *Contrib Mar Sci* 27:143–158.
- Joint Analysis Group (2010) Review of preliminary data to examine subsurface oil in the vicinity of MC252 #1: May 19 to June 19, 2010., Available at beta.w1.noaa.gov/scienceemissions/PDFs/JAG_Data_Report_Subsurface%20Oil_Final.pdf.
- Anderson V (1950) Sound scattering from a fluid sphere. *J Acoust Soc Am* 22:426–431.
- Zheng L, Yapa P (2000) Buoyant velocity of spherical and nonspherical bubbles/droplets. *J Hydraul Eng* 126:852–854.
- Committee on Oil in the Sea (2003) *Oil in the Sea III: Inputs, Fates, and Effects* (Natl Academies Press, Washington, DC) p 108.
- George A, Naura Al-Majrafi, Singh R, Arafin S (2008) Thermo-elastic and thermodynamic properties of light and heavy crude oil. *Phys Chem Liq* 46:328–341.
- Yapa P, Chen F (2004) Behavior of oil and gas from deepwater blowouts. *J Hydraul Eng* 130:540–553.